Inorganic Chemistry

Communication

pubs.acs.org/IC

Coordination-Induced Spin-State Switching with Nickel Chlorin and Nickel Isobacteriochlorin

Marcel Dommaschk,[†] Vanessa Thoms,[†] Christian Schütt,[†] Christian Näther,[‡] Rakesh Puttreddy,[§] Kari Rissanen,[§] and Rainer Herges*[,†]

[†]Otto-Diels-Institut für Organische Chemie, Christian-Albrechts-Universität, Otto-Hahn-Platz 4, D-24098 Kiel, Germany

[‡]Institut für Anorganische Chemie, Christian-Albrechts-Universität, Otto-Hahn-Platz 6/7, 24098 Kiel, Germany

[§]Department of Chemistry, Nanoscience Center, University of Jyvaskyla, P.O. Box 35, 40014 Jyvaskyla, Finland

Supporting Information

ABSTRACT: We present the first coordination-induced spin-state switching with nickel chlorin and nickel isobacteriochlorin. The spin-state switching was monitored by UV−vis spectroscopy and NMR titration experiments. The association constants (K_1 and K_2) and thermodynamic parameters (ΔH and ΔS) of the coordination of pyridine were determined. The first X-ray analyses of a paramagnetic nickel chlorin and a nickel isobacteriochlorin provide further information about the structure of the octahedral complexes. Nickel chlorin and even more pronounced nickel isobacteriochlorin exhibit stronger coordination of axial ligands compared to the corresponding nickel porphyrin and thus provide the basis for more efficient spin-switching systems.

Nickel(II) can exist in two different spin states ($S = 0$ and 1). The spin state of nickel complexes in solution is known to depend on the coordination number and geometry. A frequently used method to control the spin state is the addition of ligands to a square-planar nickel complex ($S = 0$).[1−4] Axial-ligand coordination gives rise to the formation of square-pyramidal and octahedral complexes and converts the nickel(II) to the $S = 1$ state.[5−7] This process was coined coordination-induced spin-state switching (CISSS).[8] Preconditions for the design of efficient spin-switching systems are rigid square-planar nickel complexes that allow strong coordination of axial ligands. Nickel porphyrins have proven to be suitable. With photochromic ligands, the coordination number and spin state can be controlled by irradiation with light (light-driven CISSS).[9−12] As previously shown, this process has been used to change the contrast in magnetic resonance imaging (MRI).[13,14] The square-planar complex is MRI-silent (contrast off), whereas the axial complexes are paramagnetic and active (contrast on). The CISSS approach provides the basis for the design of smart MRI contrast agents, which have a high potential for applications in functional medical imaging.

The nickel porphyrin systems that have been developed toward this end so far still suffer from drawbacks, mainly in view of medical applications. Axial coordination has to be improved, and the wavelength of light for addressing the systems in vivo has to be shifted toward the biooptical window (650−950 nm), where blood-supported tissue is transparent (penetration depth of up to 20 mm). To solve these problems, we explore the implementation of nickel chlorins and nickel isobacteriochlorins in CISSS systems because they are known to have bathochromic-shifted absorption bands compared to the corresponding porphyrins.

We started from *meso*-tetrakis(pentafluorophenyl)nickel porphyrin (Ni-TPPF$_{20}$, **1**), whose complex formation with pyridine is well investigated and which is a common platform for CISSS.[8,9,11] Chlorins and isobacteriochlorins can be prepared by the reduction of porphyrins. In the case of electron-deficient porphyrins, however, cycloaddition reactions are more convenient to convert β double bonds to C−C single bonds (Supporting Information). Hence, we applied the method of Cavaleiro et al. using *N*-methylglycine and formaldehyde in boiling toluene (Scheme 1).[15−17] The corresponding chlorin (Ni-TPCF$_{20}$, **2**) and isobacteriochlorin (Ni-TPIBF$_{20}$, **3**) were obtained with 43 and 19% yield (Supporting Information). No detectable amounts of bacteriochlorin and syn-configured isobacteriochlorin were observed, which confirms the selectivity of this reaction with the free base porphyrin.[16]

Scheme 1. Formation of 2 and 3 by the 1,3-Dipolar Cycloaddition of 1 and an Azomethine Ylide Formed in Situ by the Reaction of *N*-Methylglycine and Formaldehyde

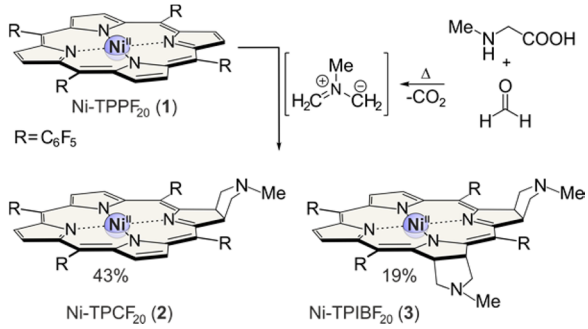

The nickel macrocycles **2** and **3** were investigated with UV−vis spectroscopy (Figure 1). The most bathochromic absorption bands (Q bands) were found at 554 nm for the porphyrin, at 596 nm for the nickel isobacteriochlorin **3**, and at 613 nm for the

Received: August 4, 2015
Published: September 24, 2015

DOI: 10.1021/acs.inorgchem.5b01756
Inorg. Chem. 2015, 54, 9390−9392

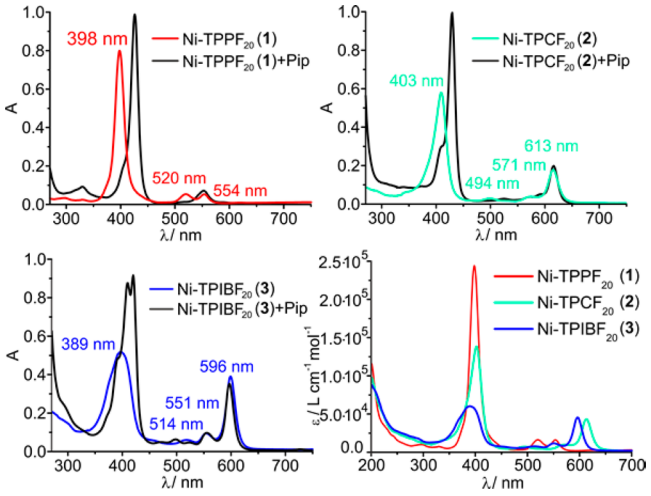

Figure 1. (top and bottom left) UV–vis spectra of compounds **1**–**3** in pure MeCN (red, green, and blue) and with an excess of piperidine in MeCN (black). (bottom right) Comparison of the extinction coefficients of compounds **1**–**3**.

nickel chlorin **2**. The latter absorption is close to the near-IR window and has a measurable absorption at >650 nm. An even larger bathochromic shift was observed for the metal-free chlorin (652 nm).[16] The extinction coefficients of the Soret bands are decreasing from **1** to **2** to **3**, in contrast to the more interesting Q bands, for which the order is in reverse (**3** to **2** to **1**). All three compounds exhibit a bathochromic shift of the Soret band upon the addition of piperidine, which is due to formation of the paramagnetic octahedral complex.[18]

The capability of a nickel complex to perform CISSS is quantified by the association constants. It is important to consider that there are two association processes. The coordination of the first axial ligand to form the paramagnetic square-pyramidal complex is described by the association constant K_1, and the coordination of the second ligand to form the octahedral complex is denoted as K_2 (Figure 2). Note that K_1 is the key parameter

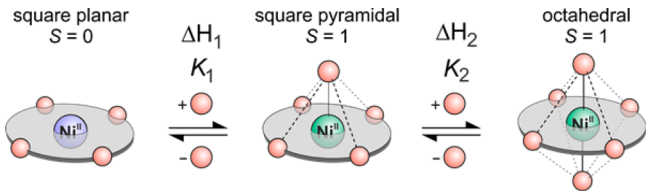

Figure 2. Formation of square-pyramidal and octahedral nickel complexes as described by the association constants (K_1 and K_2) and the complex formation enthalpies (ΔH_1 and ΔH_2).

because in this step the spin state of the nickel changes from $S = 0$ (singlet) to 1 (triplet). Whereas the two sides of **1** and **3** are homotopic, there are two different possibilities for the coordination of the first ligand to the nickel chlorin **2** (Scheme 1). According to our calculations, both 1:1 complexes (syn and anti to the pyrrolidine ring) are isoenergetic (ΔE = 0.13 kcal mol^{-1}; Supporting Information) because there is very little steric repulsion between the axial ligand and the pyrrolidine unit. Hence, we use the same binding model as that for the nickel porphyrin **1** and nickel isobacteriochlorin **3** (Figure 2).

The association constants of pyridine with the nickel porphyrin **1**, nickel chlorin **2**, and nickel isobacteriochlorin **3** were determined by ^{1}H NMR spectroscopy (toluene-d_8; see Supporting Information). Surprisingly, the key parameter for the spin switch, K_1, drastically increases with the number of saturated double bonds in the macrocycle (Table 1). The nickel

Table 1. Association Constants (K_1 and K_2; 300 K, Toluene-d_8) of Pyridine to 1,[8] 2, and 3[a]

	K_1 (L mol^{-1})	K_2 (L mol^{-1})
Ni-TPPF$_{20}$ (**1**)	7.8	20.5
Ni-TPCF$_{20}$ (**2**)	91.1	43.4
Ni-TPIBF$_{20}$ (**3**)	441.0	77.5

[a]All values and titration curves are given in the Supporting Information.

chlorin **2** binds pyridine 12 times stronger and the nickel isobacteriochlorin **3** even 57 times stronger than the nickel porphyrin **1**. Hence, nickel chlorins, and even more so nickel isobacteriochlorins, are better platforms for CISSS.

From temperature-dependent measurements of the association constants, the thermodynamic parameters (ΔH and ΔS) for complex formation were determined (Table 2). The entropies

Table 2. ΔH and ΔS Values for the Association of Pyridine to 1,[8] 2, and 3 Determined by the Temperature Dependence of the Association Constants (Supporting Information)

	ΔH_1 (kcal mol^{-1})	ΔS_1 (cal mol^{-1} K^{-1})	ΔH_2 (kcal mol^{-1})	ΔS_2 (cal mol^{-1} K^{-1})
Ni-TPPF$_{20}$ (**1**)	−5.3	−13.6	−6.0	−13.9
Ni-TPCF$_{20}$ (**2**)	−6.9	−14.1	−6.2	−13.0
Ni-TPIBF$_{20}$ (**3**)	−8.0	−14.6	−7.0	−14.9

ΔS_1 and ΔS_2 for all processes are almost equal (−13.6 to −14.9 cal mol^{-1} K^{-1}). Hence, the association enthalpies ΔH_1 and ΔH_2 exhibit the same trend as the association constants K_1 and K_2. The key parameter ΔH_1 for **1**–**3** increases more strongly than ΔH_2.

These trends are very well reproduced by quantum-chemical calculations. Previously, we have shown that the B3LYP/def2TZVP//PBE/SVP level of density functional theory (DFT) is a good compromise between the computational costs and accuracy for the calculation of binding energies in nickel porphyrins.[9,10] Table 3 compares the experimental and theoretical values for **1**–**3**. Obviously, this DFT level is also reliable for nickel chlorins and nickel isobacteriochlorins.

Table 3. Experimental (ΔH) and Theoretical (E_f) Values (B3LYP/def2TZVP//PBE/SVP) of Complex Formation Energies of 1–3 with Two Pyridine Ligands

	$\Delta H_1 + \Delta H_2$ (kcal mol^{-1})	E_f (kcal mol^{-1})
Ni-TPPF$_{20}$ (**1**)	−11.3	−10.8
Ni-TPCF$_{20}$ (**2**)	−13.1	−12.1
Ni-TPIBF$_{20}$ (**3**)	−15.0	−13.6

We were able to obtain single-crystal structures of the bis(pyridine) complexes of **1**–**3** (**1**·2Py, **2**·2Py, and **3**·2Py; Figure 3), which allows (for the first time) the direct comparison of the structures of paramagnetic nickel porphyrins and saturated analogues. As expected from the increasing binding energies in **1**–**3**, the coordinative Ni–N bond length decreases. The coordination sphere of the nickel ion in all three complexes is octahedral with tetragonal distortion (square-bipyramidal). Whereas the porphyrin unit in **1**·2Py is perfectly planar, slight

DOI: 10.1021/acs.inorgchem.5b01756
Inorg. Chem. 2015, 54, 9390–9392

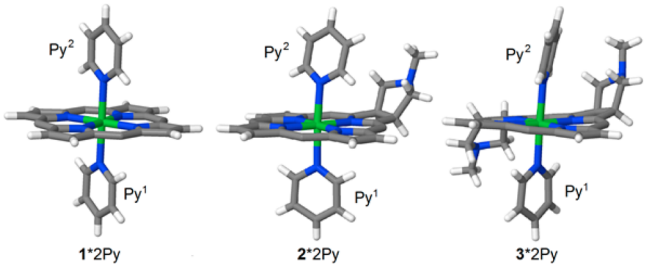

Figure 3. Single-crystal structure of octahedral complexes of the nickel porphyrin **1** (left), nickel chlorin **2** (middle), and nickel isobacteriochlorin **3** (right) with pyridine as the axial ligand. The C_6F_5 substituents at the meso positions were omitted.

ruffling is observed in chlorin **2**·2Py and is even more pronounced in isobacteriochlorin **3**·2Py, which is quantified by the maximum torsion angle between the four porphyrin nitrogen atoms (N_4 torsion; see Table 4). The axial pyridines are perfectly orthogonal to the porphyrin plane in **1**·2Py. In **2**·2Py and **3**·2Py, one of the pyridines is 10° tilted, which is probably a packing effect. The suboptimal binding angle results in a slightly increased bond length (Table 4). In **1**·2Py, the pyridines (Py^1 and Py^2) are perfectly coplanar, whereas they are twisted in **2**·2Py and are even more pronounced in **3**·2Py. Interesting structural parameters are summarized in Table 4.

Table 4. Structural Parameters of 1·2Py, 2·2Py, and 3·2Py[a]

		Ni−N bond/Å		tilt	Py^1Py^2	N_4-	space-
		crystal	calc.	angle	twist	torsion	group
1·2Py	Py^1	2.223	2.205	0°	0°	0°	P-1
	Py^2	2.223	2.205	0°			
2·2Py	Py^1	2.185	2.191	0°	20°	1.4°	$P2_1/c$
	Py^2	2.199	2.198	10°			
3·2Py	Py^1	2.181	2.185	2°	27°	3.1°	P-1
	Py^2	2.192	2.185	10°			

[a]The overlay of calculated (PBE/SVP) and crystal structure is provided in the Supporting Information.

By crystallization in the absence of pyridine, we obtained single-crystal structures of the diamagnetic nickel porphyrin **1** and a linear coordination polymer of the nickel chlorin **2**. The structures are in good agreement with the calculated structures at the PBE/SVP level of DFT (Supporting Information).

In summary, we show that nickel chlorins and nickel isobacteriochlorins are superior as square-planar platforms for CISSS compared to the corresponding nickel porphyrins. The association constants with axial ligands increase with the number of double bonds that are replaced by single bonds (porphyrin < chlorin < isobacteriochlorin). A strong coordination of the axial ligand is important for the development of water-soluble systems because the coordination strength in water is reduced by hydrogen bonding to the ligand. Moreover, the absorption is shifted to longer wavelengths. The nickel chlorin **2** has a Q band at 613 nm, which extends into the biooptical window (650−950 nm). Nickel bacteriochlorins absorb at even longer wavelengths (~700 nm) and, therefore, are our next targets.[16] Further studies are devoted toward substitution of the pyrrolidine nitrogen with photochromic azopyridine switches to prepare spin switches that can be controlled with near-IR light.[10,12,13] These compounds are interesting candidates as functional MRI contrast agents with potential applications in functional imaging and interventional radiology.[19]

■ ASSOCIATED CONTENT

Supporting Information

The Supporting Information is available free of charge on the ACS Publications website at DOI: 10.1021/acs.inorgchem.5b01756.

Experimental details, full characterization of all new compounds, data evaluation of the titration experiments, computational details, and XRD data (PDF)

CCDC 1415585 (**1**), 1415586 (**1**·2Py), 1415587 (**2**), 1407134 (**2**·2Py), and 1415588 (**3**·2Py) (CIF)

■ AUTHOR INFORMATION

Corresponding Author

*E-mail: rherges@oc.uni-kiel.de. Phone: +49 431 880 2440.

Notes

The authors declare no competing financial interest.

■ ACKNOWLEDGMENTS

This work has been supported by the Deutsche Forschungsgemeinschaft within the SFB 677 "Function by Switching" and the Academy of Finland (Grants 263256 and 265328 to K.R.).

■ REFERENCES

(1) Caughey, W. S.; Deal, R. M.; McLees, B. D.; Alben, J. O. *J. Am. Chem. Soc.* **1962**, *84*, 1735−1736.
(2) Caughey, W. S.; Fujimoto, W. Y.; Johnson, B. P. *Biochemistry* **1966**, *5*, 3830−3843.
(3) Cole, S. J.; Curthoys, G. C.; Magnusson, E. A.; Phillips, J. N. *Inorg. Chem.* **1972**, *11*, 1024−1028.
(4) McLees, B. D.; Caughey, W. S. *Biochemistry* **1968**, *7*, 642−652.
(5) Kim, D.; Su, Y. O.; Spiro, T. G. *Inorg. Chem.* **1986**, *25*, 3988−3993.
(6) Song, Y.; Haddad, R. E.; Jia, S.-L.; Hok, S.; Olmstead, M. M.; Nurco, D. J.; Schore, N. E.; Zhang, J.; Ma, J.-G.; Smith, K. M.; Gazeau, S.; Pécaut, J.; Marchon, J.-C.; Medforth, C. J.; Shelnutt, J. A. *J. Am. Chem. Soc.* **2005**, *127*, 1179−1192.
(7) Bütje, K.; Nakamoto, K. *Inorg. Chim. Acta* **1990**, *167*, 97−108.
(8) Thies, S.; Bornholdt, C.; Köhler, F.; Sönnichsen, F. D.; Näther, C.; Tuczek, F.; Herges, R. *Chem. - Eur. J.* **2010**, *16*, 10074−10083.
(9) Thies, S.; Sell, H.; Bornholdt, C.; Schütt, C.; Köhler, F.; Tuczek, F.; Herges, R. *Chem. - Eur. J.* **2012**, *18*, 16358−16368.
(10) Dommaschk, M.; Schütt, C.; Venkataramani, S.; Jana, U.; Näther, C.; Sönnichsen, F. D.; Herges, R. *Dalton Trans.* **2014**, *43*, 17395−17405.
(11) Thies, S.; Sell, H.; Schütt, C.; Bornholdt, C.; Näther, C.; Tuczek, F.; Herges, R. *J. Am. Chem. Soc.* **2011**, *133*, 16243−16250.
(12) Venkataramani, S.; Jana, U.; Dommaschk, M.; Sönnichsen, F. D.; Tuczek, F.; Herges, R. *Science* **2011**, *331*, 445−448.
(13) Dommaschk, M.; Peters, M.; Gutzeit, F.; Schütt, C.; Näther, C.; Sönnichsen, F. D.; Tiwari, S.; Riedel, C.; Boretius, S.; Herges, R. *J. Am. Chem. Soc.* **2015**, *137*, 7552−7555.
(14) Dommaschk, M.; Gutzeit, F.; Boretius, S.; Haag, R.; Herges, R. *Chem. Commun.* **2014**, *50*, 12476−12478.
(15) Silva, A. M. G.; Tomé, A. C.; Neves, M. G. P. M. S.; Silva, A. M. S.; Cavaleiro, J. A. S. *Chem. Commun.* **1999**, 1767−1768.
(16) Silva, A. M. G.; Tomé, A. C.; Neves, M. G. P. M. S.; Silva, A. M. S.; Cavaleiro, J. A. S. *J. Org. Chem.* **2005**, *70*, 2306−2314.
(17) de Souza, J. M.; de Assis, F. F.; Carvalho, C. M.; Cavaleiro, J. A.; Brocksom, T. J.; de Oliveira, K. T. *Tetrahedron Lett.* **2014**, *55*, 1491−1495.
(18) Kaplan, W. A.; Scott, R. A.; Suslick, K. S. *J. Am. Chem. Soc.* **1990**, *112*, 1283−1285.
(19) Herges, R.; Jansen, O.; Tuczek, F.; Venkatamarani, S. Molecular Switch. Patent WO 2012022299 A1, Feb 23, 2012.

DOI: 10.1021/acs.inorgchem.5b01756
Inorg. Chem. 2015, 54, 9390−9392